

Exploring multiple scales and bi-hemispheric asymmetric EEG features for emotion recognition

Yihan Wu^a, Min Xia^a, Huan Cai^a, Li Nie^a, Yangsong Zhang^{a,b,*}

^a*School of Computer Science and Technology, Southwest University of Science and Technology, Mianyang, China*

^b*Key Laboratory of Cognition and Personality, Ministry of Education, Chongqing, China*

Abstract

In recent years, emotion recognition based on electroencephalography (EEG) has received growing interest in the brain-computer interaction (BCI) field. The neuroscience researches indicate that the left and right brain hemispheres demonstrate differences under different emotional activities, which is an important principle for designing deep learning (DL) model for emotion recognition. Besides, the neural activities of emotions may occur at different time scales and duration, it is beneficial to use multiple kernels with different sizes to learn the temporal multi-scale features. Based on these two angles, we propose Multi-Scales Bi-hemispheric Asymmetric Model (MSBAM) based on a two-branch convolutional Neural Networks (CNN). We first use different kernel in two separate branch to extract distinct temporal representations, and then bi-hemispheric asymmetric feature extractor to learn asymmetric spatial features in each branch. Then, the features from the two branches are combined together for emotion state recognition. Evaluated on the public DEAP dataset, MSBAM yields accuracies over 98% on two-class classification for both valence and arousal states.

Keywords:

Emotion recognition, EEG, Deep learning, Convolutional neural networks

1. Introduction

Emotion is a kind of physiological and psychological phenomenon playing a significant role in daily life[1][2]. In recent years, emotion recognition based

*Correspondence to: YS Zhang (zhangysacademy@gmail.com)

on machine learning and deep learning methods has attracted more and more attention of the research community [3]. Emotions can be detected from different modalities, such as facial expression [4], speech [5], and physiological data [6], etc. Among these, the physiological signals are hard to fake and show a decided advantage in measurement of spontaneous mental activity under different emotion states.

Human physiological signals can be measured by different imaging modalities, such as functional magnetic resonance imaging (fMRI), magnetoencephalography (MEG), functional near-infrared spectroscopy (fNIRS), and electroencephalography (EEG), et al. Benefiting from properties such as high temporal resolution, non-invasive, low cost, and the portability of devices, EEG has been widely employed in the emotion recognition field [7].

To differentiate emotional states, the conventional approaches adopted feature extractor plus classifier mode to build the algorithms. Various hand-crafted features have been employed to extract the differences between different emotional states. For instance, Wen et al. utilized Pearson correlation coefficient (PCC) to estimate the correlation between all channel pairs [8]. Zheng et al. adopted power spectral density (PSD), differential entropy (DE), differential asymmetry (DASM), rational asymmetry (RASM), asymmetry (ASM) and differential causality (DCAU) features in their study [9]. Moon et al. employed Pearson correlation coefficient (PCC), phase-locking value (PLV) and transfer entropy (TE) to conduct their experiment [10].

With the rapid development of deep learning, increasing researchers pursue an end-to-end solution to replace the conventional classification methods based on handcraft features. Ma et al. proposed a method, which applied residual structure on long-short term memories neural networks(LSTM) [11]. Yang et al. propose parallel convolutional recurrent neural network combining of convolutional neural networks(CNN) and LSTM [12]. Yin et al. propose a method fusing graph convolutional neural networks (GCNN) and LSTM [13].

For the past few years, increasing studies have started to design the DL models by considering the physiological mechanisms of emotion. Bi-hemispheric discrepancy under different emotion states is a vital neural mechanism, which has been used in several studies with DL model for emotion recognition [14, 15]. For instance, Li et al. proposed a method termed as R2G-STNN [16]. They extracted regional features according to the spatial region concerning physiological function, and fused the regional and global features. In another study, Li et al. proposed a method using LSTM to

capture the features of bi-hemispheric discrepancy [14].

EEG signals carry information at different time scales and duration, it is beneficial for DL model to use multiple kernels with different sizes to learn the multi-scale temporal features [17]. For example, Li et al. proposed a multi-scale fusion CNN model for motor imagery classification [18]. The experimental results indicated that the model achieved a better performance compared with the baseline methods. The multi-scale CNN has also been introduced in emotion recognition. Phan et al. proposed a 2D CNN model with Multi-Scale Kernels for arousal and valence binary classification [19].

However, the physiological mechanisms and multi-scale features of EEG has not been simultaneously considered in a DL model. Based on this consideration, we propose DL model termed Multi-Scales Bi-hemispheric Asymmetric Model (MSBAM). We first use different kernel in distinct branches to extract various temporal representations, and then bi-hemispheric asymmetric feature extractor to learn asymmetric spatial features. The MSBAM could capture the correlation among temporal information by employing multiple extractors with different scales, and then combining bi-hemispheric discrepant features to obtain better performance. We conduct experiments on DEAP dataset, which proves our MSBAM has superior average accuracy than all the traditional baseline methods.

The remainder of this paper is organized as follows. Section 2 introduces Materials and Methods. Section 3 describes the settings and results of extensive experiments, comparisons between MSBAM and the baseline methods are also be provided in this section. Section4 and 5 present the discussions and conclusion.

2. Materials and Methods

2.1. DEAP dataset

To validate the performance of our MSBAM, we use the DEAP dataset, which is the most widely used in emotion recognition domain. The DEAP dataset is a multimodal dataset first presented by Koelstra and colleagues[20]. Thirty-two healthy subjects participated in the experiment. They were watching 40 pieces of music videos for one-minute long. The electroencephalogram (EEG) and peripheral physiological signals were recorded when they were watching videos. Forty electrodes(32 for EEG and 8 for peripheral physiological signals) are applied in the recording, and all the electrodes conform with the international standard 10-20 system. Participants were asked

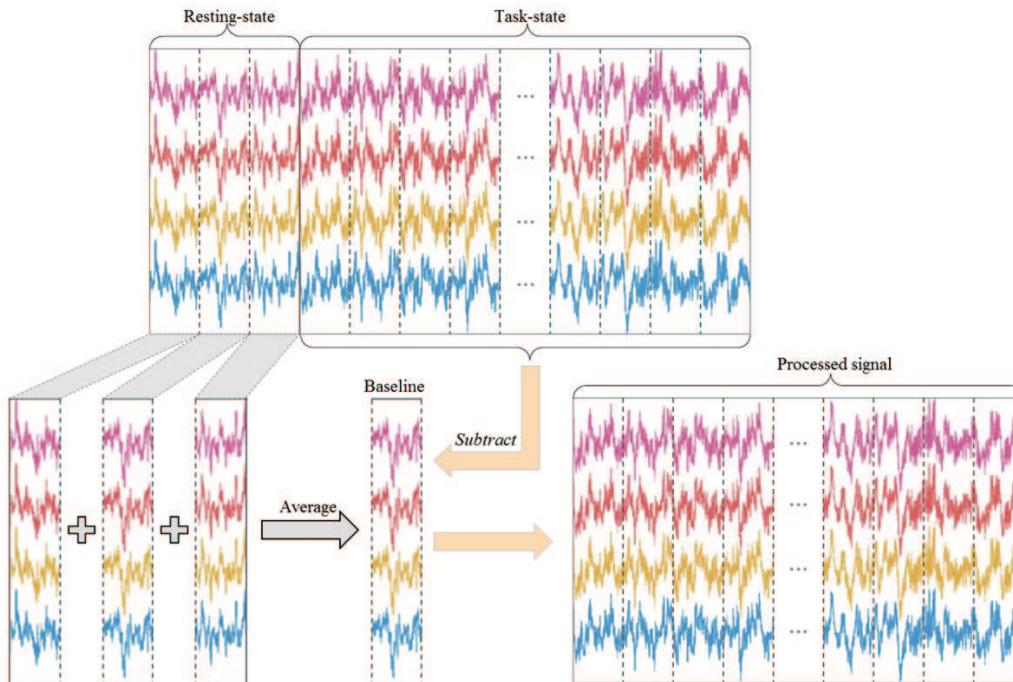


Figure 1: The diagram of baseline correction for DEAP dataset. The first 3 seconds is regarded as resting-state data. All the task-state data should subtract the average signal of resting-state second by second.

to rate each video from 1 to 9 to evaluate the levels of arousal, valence, liking, dominance and familiarity. Each trial contains 3 s baseline data and 60 s experimental data. The EEG signals were down-sampled to 128 Hz from 512 Hz, and averaged to the common reference. Electro-oculogram (EOG) artefacts were removed. A bandpass frequency filter was implemented from 4-45 Hz. The details can be found in the reference [20].

The class label in the DEAP dataset for each dimension is from 1 to 9. For the two-class classification, labels of the data in the *valence* and *arousal* states are set to low and high by the threshold of score 5, respectively.

2.2. Data processing

In order to reduce the noise and improve the stability of the signal, baseline correction and z-score normalization, which were commonly pre-processing procedures for EEG, were implemented on the dataset.

Previous studies demonstrated that these operations can improve emotion

recognition accuracy by reducing the interference of basic emotional state without any stimulation [21]. The diagram of baseline correction is illustrated in the Fig. 1.

First, the 3 s baseline data were divided into three segments of 1 s length without overlap. These segments were further averaged to obtain the baseline signal of 1 s length, termed as resting-state segment. Second, the 60 s trial data were also divided into 60 segments of 1 s length without overlap, termed as task-state segments. Third, each task-state segment was subtracted by the resting-state segment, and then normalized with z-score normalization. After these steps, we concatenated all the processed task-state segments to construct the task-state data of 60 s.

After the preprocessing procedure, the new task-state will be segmented with Wnd seconds window without overlap. Finally, we get samples $D \in \mathbb{R}^{C \times T}$, where C denotes the number of channels and $T = Fs \times Wnd$ represents the sample points. Fs denotes the sampling rate which has been down sampled to 128.

Due to having multiple temporal extractors, MSBAM has extraordinary sensitivity about the length of sliding window. We set the parameter Wnd to be 5 in the following experiments.

2.3. 3D representation

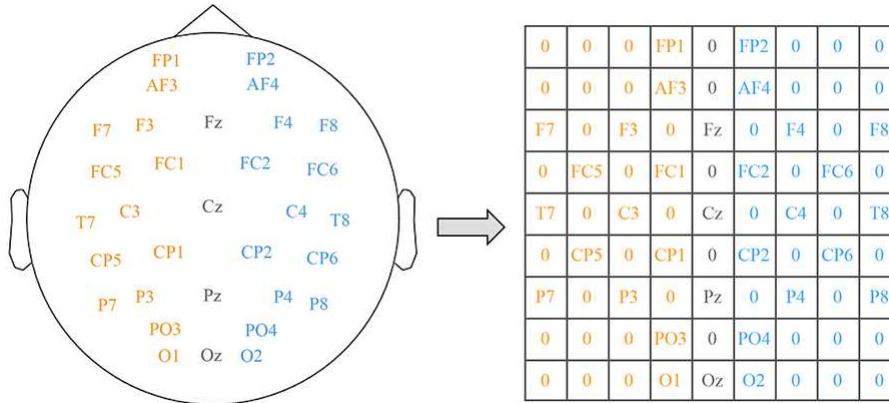


Figure 2: A schematic diagram of a 2D representation of EEG channel locations with a 9×9 matrix.

Traditionally, EEG data is represented as 2D matrix with the shape of channels \times sample points for most algorithms. By the method of 2D rep-

resentation, the data from all used channels at a sampling time point are arranged into a column vector, which lose the relative spatial position information among different channels. In recent years, the 3D representation has been introduced for EEG data [22]. In this way, the data from all used channels at one sample point are arranged into a 2D matrix according to distribution of electrodes, which can retain the spatial information among channels to some extent. We denote this operation as spatial transformation. The schematic diagram is shown in Fig. 2. We implement the spatial transformation at all sample points. Then, we can obtain the 3D representation of the EEG data. This 3D representation can preserve both temporal information and spatial information for EEG data, which has been adopted for various EEG classification tasks [23, 24].

As the input of our model, each sample $D \in \mathbb{R}^{C \times T}$ was transformed to a 3D spatial-temporal matrix $D \in \mathbb{R}^{H \times W \times T}$. In current study, $C = 32$, $T = 640$, and H and W are set to 9.

2.4. The construction of proposed MSBAM

Previous studies indicate the import roles of the physiological mechanisms and multi-scale features of EEG for emotion recognition [14, 19]. However, these two factors have not been simultaneously considered in a DL model for emotion recognition. Therefore, we proposed a MSBAM model based on the CNN. The MSBAM contains three parts, i.e., the input layer, a bi-hemispheric asymmetric feature extractor block, and a feature concatenation and classification block. The structure is shown in Fig. 3(a).

2.4.1. Bi-hemispheric asymmetric feature extractor block

For the bi-hemispheric asymmetric feature extractor block, as is shown in Fig. 3(b), it contains two branches (Feature extractor 1, Feature extractor 2), each of which contains a convolution layer (Conv), a full-connection layer (FC), and concatenation and flatten operations.

In each branch, the EEG data D are input into the Conv layer firstly. The Conv operator named $E_{conv}(\cdot)$ has a 3D filter with 16 kernels of size $9 \times 5 \times T$, and of stride $9 \times 4 \times S$, where the T is the time scale of the extractor, and the S is equal to $T/2$. This filter could extract continuous 16 bi-hemispheric features, which could be described as:

$$F_{conv} = E_{conv}(D) \in \mathbb{R}^{1 \times 2 \times \hat{L}} \quad (1)$$

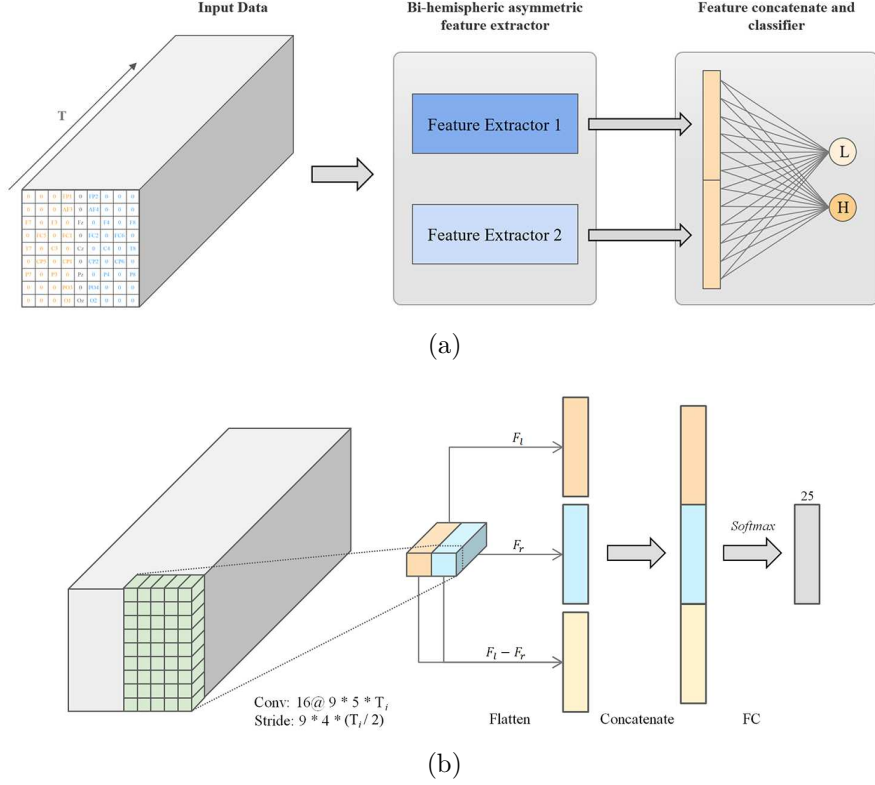


Figure 3: (a) shows overall structure of the proposed MSBAM. (b) shows the i -th bi-hemispheric asymmetric feature extractor.

where the \hat{L} are equal to $((L-T)//S + 1)$. Then, ELU activation and batch normalization are utilized.

After Conv layer, the features F_{conv} will be divided into two parts along the second dimension, $F_l \in \mathbb{R}^{1 \times 1 \times \hat{L}}$ and $F_r \in \mathbb{R}^{1 \times 1 \times \hat{L}}$. $F_{conv} = [F_l \parallel F_r]$, where the \parallel means concatenation operation. F_l and F_r are used to represent the features from left and the right hemispheres, respectively. Then, the asymmetric features between two hemispheres $F_a \in \mathbb{R}^{1 \times 1 \times \hat{L}}$, could be calculated with F_l and F_r . The calculation is described as following:

$$F_a = F_l - F_r \quad (2)$$

After that, these three kinds of features, i.e., F_l , F_r and F_a , are first flattened to vectors ($V_l \in \mathbb{R}^{\hat{L}}$, $V_r \in \mathbb{R}^{\hat{L}}$, and $V_a \in \mathbb{R}^{\hat{L}}$), further combined into

a vector $V_{cat} \in \mathbb{R}^{\hat{L}*3}$ with following operations:

$$\begin{aligned} V_l &= Flatten(F_l) \\ V_r &= Flatten(F_r) \\ V_a &= Flatten(F_a) \\ V_{cat} &= [V_l \parallel V_r \parallel V_a] \end{aligned} \quad (3)$$

Then, the feature V_{cat} is input into a fully connected layer with softmax activation to obtain the final feature V_{afe} , which could be described as:

$$V_{linear} = W \cdot V_{cat} + b = [V_1, V_2, \dots, V_{25}] \in \mathbb{R}^{25} \quad (4)$$

$$\begin{aligned} \bar{V}_i &= \frac{\exp(V_i)}{\sum_{k=1}^{25} \exp(V_k)}, i = 1, 2, \dots, 25 \\ \bar{S} &= [\bar{V}_1, \bar{V}_2, \dots, \bar{V}_{25}] \in \mathbb{R}^{25} \end{aligned} \quad (5)$$

where the W is weight matrix, b is bias.

After these procedures above, we obtain the bi-hemispheric features at one time scale. For every sample D , we apply the Feature extractor 1 and Feature extractor 2 to obtain the related features in different time scales.

2.4.2. Feature concatenation and classification block

Through the bi-hemispheric asymmetric feature extractor block, we obtain two groups of features, denoted as \bar{S}^1, \bar{S}^2 . These features are first concatenated to a integrated vector by a concatenate layer, and followed by a dense layer of two neurons with Softmax activation function.

$$S_{cat} = [\bar{S}^1 \parallel \bar{S}^2] \in \mathbb{R}^{50} \quad (6)$$

where the \parallel denotes concatenation operation. The feature S_{cat} , which is called final feature map, will be used to visualize the model.

The predicted label of EEG data D is the class which has maximal possibility, which could be described as:

$$y_{pred} = \arg \max_c P(c|D) \quad (7)$$

where the $P(c|D)$ is the possibility of D belonging to the c -th class.

2.5. Baseline methods

To verify the performance of our model, we compared the MSBAM with 10 baseline methods. These methods are introduced briefly as follows:

The method of Tang-2017. Tang et al. proposed a model named Bimodal-LSTM. DE features are extracted from four bands of EEG signals. As for peripheral physiological features, six temporal statistics are calculated to describe the time-domain features. Both the two group of features are input in two LSTM networks respectively and concatenated as one feature matrix. The feature map is classified by a linear SVM with a hinge loss.

The method of Liu-2016. Liu et al. proposed their method including a feature extractor named Bimodal Deep Auto Encoder(BDAE) and a linear SVM classifier. The peripheral physiological signals in the dataset and Power Spectral Density (PSD) and Differential Entropy (DE) features of the EEG signals are fed into a Restricted Boltzmann Machines(RBM) to extract their features respectively. The two group of features are concatenated and input into another RBM to obtain the high-level features. Then unfold the stacked RBMs to reconstruct input features. In the end, a linear SVM is utilized to finish the emotion classification task.

The method of Liu-2019. Liu et al. introduced a method named deep canonical correlation analysis(DCCA). The raw EEG signals and peripheral physiological features are transformed by different nonlinear networks respectively. The two groups of features are fused by a weighted sum method after being regularized with the traditional CCA method. Then they use the fused features to train a linear SVM classifier.

The method of Qiu-2018. Qiu et al. proposed a multimodal emotion recognition method named Correlated Attention Network (CAN) in 2018. They extracted features with two Bidirectional Gated Recurrent Unit (GRU) neural networks. And then applied a canonical correlation to calculate the correlation. In the end, attention mechanism was utilized to implement the emotion classification task.

The method of Yin-2021. Yin et al. proposed ECLGCNN which fused LSTM and GCNN for emotion classification. In their GCNN model, the EEG channels and functional relationship between two channels are denoted as the vertex node and the edge respectively. The greater value of the edge means the relationship between two channels is closer. The features extracted by the GCNNs are input into LSTM networks to extract the higher level features for emotion classification tasks.

The method of Yang-2018. Yang et al. introduced a baseline removing pre-processing method and validated it with their new model, which is called Parallel Convolutional Recurrent Neural Network (PCRNN). The pre-processed 2D EEG signals are transformed into 3D according to the spatial topology of electrodes. Then a group of CNNs and LSTMs are utilized to extract the spatial and temporal features respectively. To classify the emotion state, features are concatenated and input into a fully connected layer.

The method of Liao-2020. Liao et al. proposed a multimodal emotion recognition method in 2020. They transform the raw EEG signal into 3D as Yang et al. did. 2D-CNNs are employed to extract the spatial features of EEG signals and LSTM are utilized to extract the temporal features of peripheral physiological signals. The concatenated spatial and temporal features are fed into a softmax classifier to predict the emotion states.

The method of Ma-2019. Ma et al. proposed a method named MMResLSTM based on EEG and peripheral physiological signals. MMResLSTM contains four LSTMs, and the last three of them have a residual structure. Multimodal data is fed into two weights shared MMResLSTM to extract the high-level features and concatenated to predict the emotion state by a softmax layer.

The method of Huang-2021. Huang et al. released a method based on the discrepancy of emotional response between two hemispheres, which is named Bi-hemisphere Discrepancy Convolutional Neural Network (BiDCNN). Three different matrices are constructed and input into the BiDCNN to extract the spatial and temporal features, including the discrepancy features of emotional responses between left and right hemispheres. In the end, all the features are concatenated and fed into a series of CNNs and dense layers to predict the emotion state.

The method of Cui-2020. Cui et al. proposed a method named Regional-Asymmetric Convolutional Neural Network (RACNN). They transform the 2D signals into 3D as Yang et al. did as well, and compress the temporal information by a 1*1 convolution layer. Then regional and asymmetric feature extractors are employed separately to extract the local and bi-hemisphere discrepancy features. These features are concatenated and fed into a multiple layer perceptron to finish the classification task.

2.6. Model implementation

For the MSBAM, the cross-entropy was employed as the loss function. Adam optimizer was utilized to minimize the loss function with 0.0001 learn-

ing rate initially. To prevent overfitting, a dropout layer with the drop rate of 0.7 was added before all of the dense layers in the model. For utilizing the experiment, $\{128, 64\}$ was used for time scales of bi-hemispheric asymmetric feature extractor.

For each subject, the 10-fold cross validation was used for emotion recognition. Average accuracy was used to evaluate the performance of the MSBAM and baseline models.

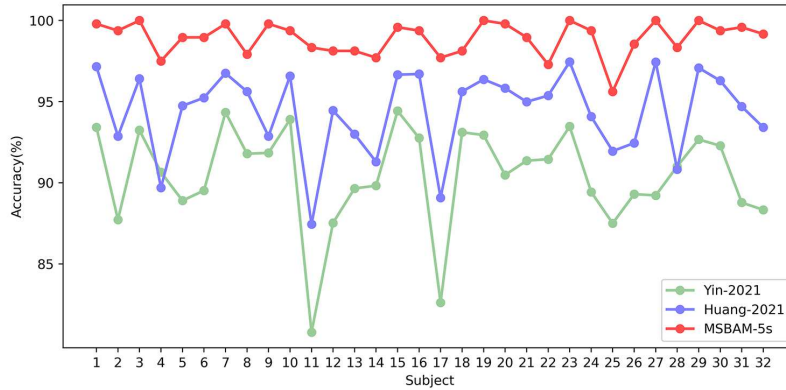
3. Results

Table 1: Accuracies of the MSBAM and other baseline methods (mean \pm std.). The symbol “/” means std. value of the method is lacking.

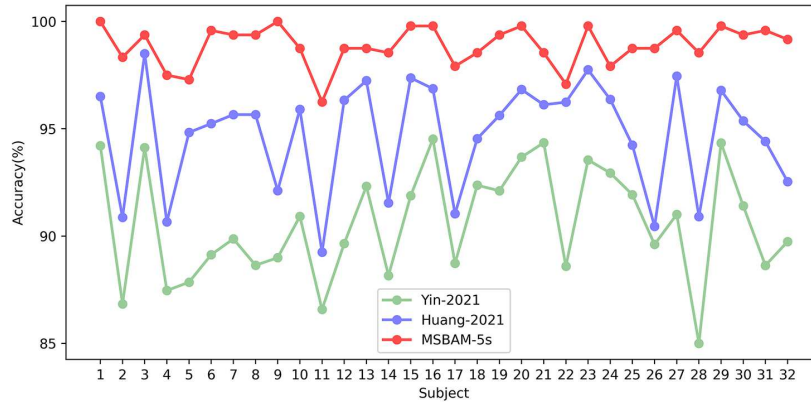
Methods	Valence(%)	Arousal(%)
Tang-2017[25]	83.82 ± 5.01	83.23 ± 2.61
Liu-2016[26]	85.20 ± 4.47	80.50 ± 3.39
Liu-2019[27]	85.62 ± 3.48	84.33 ± 2.25
Qiu-2018[28]	$86.45 \pm /$	$84.79 \pm /$
Yin-2021[29]	90.45 ± 3.09	90.60 ± 2.62
Yang-2018[30]	90.80 ± 3.08	91.03 ± 2.99
Liao-2020[31]	$91.95 \pm /$	$93.06 \pm /$
Ma-2019[32]	92.30 ± 1.55	92.87 ± 2.11
Huang-2021[15]	94.38 ± 2.61	94.72 ± 2.56
Cui-2020[23]	96.65 ± 2.65	97.11 ± 2.01
MSBAM	98.89 ± 1.03	98.87 ± 0.92

We conduct the experiments on *valence* and *arousal* dimensions to verify the effectiveness of our MSBAM, and compare the performance among different methods. The experimental results of all methods are summarized in Table 1. We could find that our MSBAM yields better performance than the baseline methods. Compared with the best baseline model, MSBAM could improve average recognition accuracy by 2.24% and 1.76% on *Valence* and *Arousal* dimensions. In addition, MSBAM achieves smallest standard deviation in all the listed methods. It means that MSBAM has better robustness than the baseline methods.

To observe the performance of proposed MSBAM on each subject, two line charts Fig. 4(a) and Fig. 4(b) are presented. In the chart, Cui-2020 is absent due to lacking of the accuracy information for each subject in the original paper [23]. We could find that all the methods yield analogical tendencies as the subject changes. The MSBAM show better performance than other models. It has the best accuracy on every subject.



(a)



(b)

Figure 4: Average for every subject on *Valence*(a) and *Arousal*(b) dimension.

We also drawn a t-SNE[33] figure to visualize the feature before the last FC layer, called final feature map, on *Valence* dimension. Four subjects with lowest accuracies were selected. The features of t-SNE are shown in Fig. 5. We employ the input data used in our method to plot the *Raw Data* in the

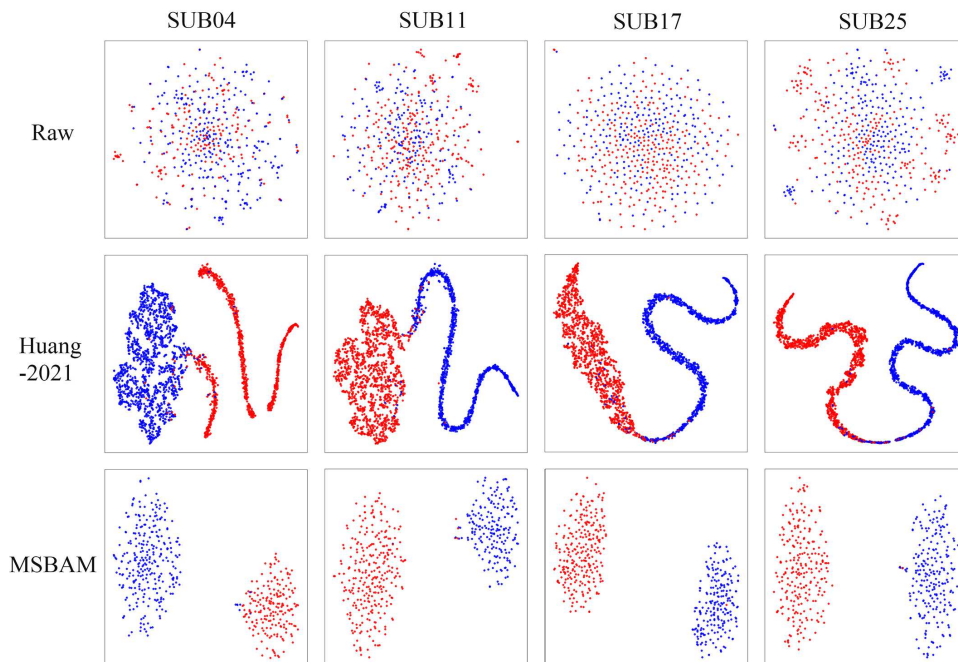


Figure 5: Visualization of the final feature maps using t-SNE. The final feature map is the feature before the last FC layer(e.g. the S_{cat} in the proposed MSBAM).

first row in Fig. 5. Because of lacking related information in the paper, we re-produced the method using the same hyper-parameter with our MSBAM and plotted the figures shown in the third row in Fig. 5. We could observe that the proposed MSBAM have better intra-category similarity and inter-category separability.

4. Discussions

The experimental results demonstrate that the proposed MSBAM model outperforms other baseline methods. This may be attributed to the model structure that simultaneously extracts the features of multi-scale and bi-hemispheric asymmetry. To further verify the rationality of the MSBAM, several ablation experiments were further conducted. We need to check that two branches in the bi-hemispheric asymmetric feature extractor block are appropriate.

First, we removed the Feature extractor 1, Feature extractor 2, respectively. The average accuracies are shown in Tables 2. MSBAM- r_i means that only the i -th extractor is kept in the original MSBAM. From the table, we could find that two branches in the MSBAM are necessary.

Table 2: Average accuracy(%) of the multi-scales ablation experiments(mean \pm std.).

Methods	Valence(%)	Arousal(%)
MSBAM-r1	97.72 \pm 1.76	95.29 \pm 5.55
MSBAM-r2	97.95 \pm 2.01	95.36 \pm 5.79
MSBAM	98.89 \pm 1.03	98.87 \pm 0.92

Table 3: Average accuracy of the model with various number of branches(mean \pm std.).

Methods	Valence(%)	Arousal(%)
MSBAM-b3	98.79 \pm 1.21	99.13 \pm 0.98
MSBAM-b4	98.73 \pm 1.25	98.93 \pm 1.03
MSBAM	98.89 \pm 1.03	98.87 \pm 0.92

Second, we added more branches into the MSBAM. In Table 3, the setting of those experiments are illustrated briefly as follows:

1) MSBAM-b3 denotes that there are 3 branches in the model. One branch with $T = 32$ is added.

2) MSBAM-b4 denotes that there are 4 branches in the model. Two branches with $T = 32$ and $T = 16$ are added.

The results of experiments demonstrate that adding more scales cannot obviously improve performance of the original model. To save the computational resource, two branches is enough for the MSBAM.

In addition, to validate the effectiveness of asymmetric features and the length of slide window, two experiments are utilized as well. The average accuracy is shown in TABLE 4. MSBAM-asy means that the asymmetric feature extractors are replaced with a convolution layer. The convolution layer has 16 kernels, and the kernel size and stride are 3*3. MSBAM-1s means that length of slide window is changed to 1 second.

The result of MSBAM-asy shows that the asymmetric features are important to improve the performance of the model, and the MSBAM-1s indicates

Table 4: Average accuracy of the model with asymmetric features replaced and length of the slide window changed.

Methods	Valence(%)	Arousal(%)
MSBAM-asy	95.83 ± 3.30	96.19 ± 2.73
MSBAM-1s	95.01 ± 1.70	95.45 ± 2.03
MSBAM	98.89 ± 1.03	98.87 ± 0.92

that the longer slide window has a great superiority for our method. We suppose that the multi-scales structure give MSBAM sensitivity in temporal dimension. It makes MSBAM capturing more effective features than MSBAM-1s. In addition, larger time scales for extractor may capture more continuous and long stride relevant feature, which is benefit for emotion recognition task.

Although performs better than all the baseline methods, the MSBAM still has several defects could be optimized. In current study, only the DEAP dataset was adopted to evaluate the performance, more datasets should be used to verify the effectiveness of the proposed MSBAM. Besides, In Table 1, we could find that all methods can obtain accuracy above 80%. However, there exists a problem of data leakage because of the approach to obtain the training data and test data trial-dependent method, which is a common phenomenon in existing DL models. Few studies try to evaluate the DL models on more challenging scenarios, trial-independent classification within subject and subject-independent classification [34]. These two scenarios should be adopted in future studies when we evaluate the DL models to avoid data leakage and biased evaluation.

5. Conclusion

In this paper, we propose an emotion recognition method based on multi-scale and bi-hemispheric asymmetric features, named MSBAM. The proposed MSBAM could achieve average accuracies of 98.89% and 98.87% on *Valence* and *Arousal* dimensions respectively, which outperform all the baseline methods. Although some limitations should be addressed in future studies, current study demonstrates that multi-scale and bi-hemispheric Asymmetric EEG features are beneficial for emotion recognition.

References

- [1] R. J. Dolan, Emotion, cognition, and behavior, *Science* 298 (5596) (2002) 1191–1194.
- [2] M. Cabanac, What is emotion?, *Behavioural Processes* 60 (2) (2002) 69–83.
- [3] E. P. Torres, E. A. Torres, M. Hernández-Álvarez, S. G. Yoo, Eeg-based bci emotion recognition: a survey, *Sensors* 20 (18) (2020) 5083.
- [4] S. Zhao, H. Tao, Y. Zhang, T. Xu, K. Zhang, Z. Hao, E. Chen, A two-stage 3d cnn based learning method for spontaneous micro-expression recognition, *Neurocomputing* 448 (2021) 276–289.
- [5] M. El Ayadi, M. S. Kamel, F. Karray, Survey on speech emotion recognition: Features, classification schemes, and databases, *Pattern Recognition* 44 (3) (2011) 572–587.
- [6] P. Li, H. Liu, Y. Si, C. Li, F. Li, X. Zhu, X. Huang, Y. Zeng, D. Yao, Y. Zhang, P. Xu, Eeg based emotion recognition by combining functional connectivity network and local activations, *IEEE Transactions on Biomedical Engineering* 66 (10) (2019) 2869–2881. doi:10.1109/TBME.2019.2897651.
- [7] W. Li, W. Huan, B. Hou, Y. Tian, Z. Zhang, A. Song, Can emotion be transferred? – a review on transfer learning for eeg-based emotion recognition, *IEEE Transactions on Cognitive and Developmental Systems* (2021) 1–1doi:10.1109/TCDS.2021.3098842.
- [8] Z. Wen, R. Xu, J. Du, A novel convolutional neural networks for emotion recognition based on eeg signal, in: 2017 International Conference on Security, Pattern Analysis, and Cybernetics (SPAC), 2017, pp. 672–677. doi:10.1109/SPAC.2017.8304360.
- [9] W.-L. Zheng, J.-Y. Zhu, B.-L. Lu, Identifying stable patterns over time for emotion recognition from eeg, *IEEE Transactions on Affective Computing* 10 (3) (2019) 417–429. doi:10.1109/TAFFC.2017.2712143.
- [10] S.-E. Moon, C.-J. Chen, C.-J. Hsieh, J.-L. Wang, J.-S. Lee, Emotional eeg classification using connectivity features and convolutional neural networks, *Neural Networks* 132 (2020) 96–107.

- [11] J. Ma, H. Tang, W.-L. Zheng, B.-L. Lu, Emotion recognition using multimodal residual lstm network, in: Proceedings of the 27th ACM International Conference on Multimedia, MM '19, Association for Computing Machinery, New York, NY, USA, 2019, p. 176–183.
- [12] Y. Yang, Q. Wu, M. Qiu, Y. Wang, X. Chen, Emotion recognition from multi-channel eeg through parallel convolutional recurrent neural network, in: 2018 International Joint Conference on Neural Networks (IJCNN), 2018, pp. 1–7. doi:10.1109/IJCNN.2018.8489331.
- [13] Y. Yin, X. Zheng, B. Hu, Y. Zhang, X. Cui, Eeg emotion recognition using fusion model of graph convolutional neural networks and lstm, Applied Soft Computing 100 (2021) 106954.
- [14] Y. Li, W. Zheng, Y. Zong, Z. Cui, T. Zhang, X. Zhou, A bi-hemisphere domain adversarial neural network model for eeg emotion recognition, IEEE Transactions on Affective Computing 12 (2) (2021) 494–504. doi:10.1109/TAFFC.2018.2885474.
- [15] D. Huang, S. Chen, C. Liu, L. Zheng, Z. Tian, D. Jiang, Differences first in asymmetric brain: A bi-hemisphere discrepancy convolutional neural network for eeg emotion recognition, Neurocomputing 448 (2021) 140–151.
- [16] Y. Li, W. Zheng, L. Wang, Y. Zong, Z. Cui, From regional to global brain: A novel hierarchical spatial-temporal neural network model for eeg emotion recognition, IEEE Transactions on Affective Computing (2019) 1–1doi:10.1109/TAFFC.2019.2922912.
- [17] W. Ko, E. Jeon, S. Jeong, H.-I. Suk, Multi-scale neural network for eeg representation learning in bci, IEEE Computational Intelligence Magazine 16 (2) (2021) 31–45. doi:10.1109/MCI.2021.3061875.
- [18] D. Li, J. Xu, J. Wang, X. Fang, Y. Ji, A multi-scale fusion convolutional neural network based on attention mechanism for the visualization analysis of eeg signals decoding, IEEE Transactions on Neural Systems and Rehabilitation Engineering 28 (12) (2020) 2615–2626. doi:10.1109/TNSRE.2020.3037326.

- [19] T.-D.-T. Phan, S.-H. Kim, H.-J. Yang, G.-S. Lee, Eeg-based emotion recognition by convolutional neural network with multi-scale kernels, *Sensors* 21 (15) (2021).
- [20] S. Koelstra, C. Muhl, M. Soleymani, J.-S. Lee, A. Yazdani, T. Ebrahimi, T. Pun, A. Nijholt, I. Patras, Deap: A database for emotion analysis ;using physiological signals, *IEEE Transactions on Affective Computing* 3 (1) (2012) 18–31.
- [21] Y. Yang, Q. Wu, M. Qiu, Y. Wang, X. Chen, Emotion recognition from multi-channel eeg through parallel convolutional recurrent neural network, in: *2018 International Joint Conference on Neural Networks (IJCNN)*, 2018, pp. 1–7. doi:10.1109/IJCNN.2018.8489331.
- [22] X. Zhao, H. Zhang, G. Zhu, F. You, S. Kuang, L. Sun, A multi-branch 3d convolutional neural network for eeg-based motor imagery classification, *IEEE Transactions on Neural Systems and Rehabilitation Engineering* 27 (10) (2019) 2164–2177.
- [23] H. Cui, A. Liu, X. Zhang, X. Chen, K. Wang, X. Chen, Eeg-based emotion recognition using an end-to-end regional-asymmetric convolutional neural network, *Knowledge-Based Systems* 205 (2020) 106243.
- [24] Y. Zhang, H. Cai, L. Nie, P. Xu, S. Zhao, C. Guan, An end-to-end 3d convolutional neural network for decoding attentive mental state, *Neural Networks* 144 (2021) 129–137.
- [25] H. Tang, W. Liu, W.-L. Zheng, B.-L. Lu, Multimodal emotion recognition using deep neural networks, in: D. Liu, S. Xie, Y. Li, D. Zhao, E.-S. M. El-Alfy (Eds.), *Neural Information Processing*, Springer International Publishing, Cham, 2017, pp. 811–819.
- [26] W. Liu, W.-L. Zheng, B.-L. Lu, Emotion recognition using multimodal deep learning, in: A. Hirose, S. Ozawa, K. Doya, K. Ikeda, M. Lee, D. Liu (Eds.), *Neural Information Processing*, Springer International Publishing, Cham, 2016, pp. 521–529.
- [27] W. Liu, J.-L. Qiu, W.-L. Zheng, B.-L. Lu, Multimodal emotion recognition using deep canonical correlation analysis (2019). arXiv:1908.05349.

- [28] J.-L. Qiu, X.-Y. Li, K. Hu, Correlated attention networks for multimodal emotion recognition, in: 2018 IEEE International Conference on Bioinformatics and Biomedicine (BIBM), 2018, pp. 2656–2660. doi:10.1109/BIBM.2018.8621129.
- [29] Y. Yin, X. Zheng, B. Hu, Y. Zhang, X. Cui, Eeg emotion recognition using fusion model of graph convolutional neural networks and lstm, *Applied Soft Computing* 100 (2021) 106954.
- [30] Y. Yang, Q. Wu, M. Qiu, Y. Wang, X. Chen, Emotion recognition from multi-channel eeg through parallel convolutional recurrent neural network, in: 2018 International Joint Conference on Neural Networks (IJCNN), 2018, pp. 1–7. doi:10.1109/IJCNN.2018.8489331.
- [31] J. Liao, Q. Zhong, Y. Zhu, D. Cai, Multimodal physiological signal emotion recognition based on convolutional recurrent neural network, *IOP Conference Series: Materials Science and Engineering* 782 (2020) 032005. doi:10.1088/1757-899x/782/3/032005.
- [32] J. Ma, H. Tang, W.-L. Zheng, B.-L. Lu, Emotion recognition using multimodal residual lstm network, in: Proceedings of the 27th ACM International Conference on Multimedia, MM '19, Association for Computing Machinery, New York, NY, USA, 2019, p. 176–183.
- [33] L. Van der Maaten, G. Hinton, Visualizing data using t-sne., *Journal of machine learning research* 9 (11) (2008) 2579–2605.
- [34] Y. Ding, N. Robinson, Q. Zeng, C. Guan, Tsception: Capturing temporal dynamics and spatial asymmetry from eeg for emotion recognition (2021). arXiv:2104.02935.